Manuscript prepared for Clim. Past
with version 2015/04/24 7.83 Copernicus papers of the LaTeX class copernicus.cls.
Date: 2 February 2016

1200 years of warm-season temperature variability in central Scandinavia inferred from tree-ring density

P. Zhang[1], H. W. Linderholm[1], B. E. Gunnarson[2], J. Björklund[3], and D. Chen[1]

[1]Regional Climate Group, Department of Earth Sciences, University of Gothenburg, Gothenburg, Sweden
[2]Bert Bolin Centre for Climate Research, Department of Physical Geography, Stockholm University, Stockholm, Sweden
[3]Swiss Federal Research Institute WSL, Birmensdorf, Switzerland

Correspondence to: P. Zhang (peng.zhang@gvc.gu.se)

Abstract.

Despite the emergence of new high-resolution temperature reconstructions around the world, only a few cover the Medieval Climate Anomaly (MCA). Improved understanding of the spatiotemporal characteristics of the MCA is important in terms of understanding how local temperatures keep a high level under natural-forcing conditions. Here we present a new Scots pine tree-ring density based reconstruction of warm-season (April–September) temperature for central Scandinavia, called C-Scan, back to 850 CE, extending the previous one by 250 years. C-Scan is largely based on pine trees collected in a confined mountain region, where the samples were adjusted for differences in altitude and local environment, and standardised in order to preserve as much mid- and long-term temperature change as possible. C-Scan suggests that the warm peak of MCA occurred in ca. 1000–1100 CE, and points to a Little Ice Age (LIA) between 1550 and 1900 CE. Moreover, during the past millennium the coldest decades were found around 1600 CE, and the warmest 10, 30 and 100 years occurred in the most recent century. By comparing C-Scan with other millennium-long temperature reconstructions from Fennoscandia, regional differences in multi-decadal temperature variability, especially during the warm period of the last millennium were revealed. Although these differences could be due to methodological reasons, they may indicate asynchronous warming patterns across Fennoscandia. Further investigation of these regional differences and the reasons/mechanisms behind them are needed.

1 Introduction

In order to assess the role of human activities on the current climate change (Bindoff et al., 2013), numerous efforts have been made to put the present warming in a long-term context (e.g., Wilson et al., 2016). Despite these attempts, there are still some controversies about past climate. For example, global mean temperature may have been as high as in the present around one thousand years ago, during the so-called Medieval Climate Anomaly (MCA; Lamb , 1969; Grove and Switsur , 1994). However, this has been questioned since regional temperature reconstructions display large variability in timing as well as magnitude of the MCA (PAGES 2k Consortium , 2013). To further improve our understanding of past climate changes, there is still a great need to produce and improve empirical proxy data.

Tree-rings are widely recognized as excellent proxies of growing-season temperatures due to their annual resolution and absolute dating (Briffa et al., 2001). The high latitude region of Fennoscandia in northwestern Europe has a strong tradition in dendrochronological research, and its large tracts of relatively accessible boreal forests with some of the world's most temperature sensitive conifers (George , 2014) and favourable preserving conditions of dead wood (see below), make the region well suited for development of tree-ring chronologies extending back over the past millennia (Linderholm et al., 2010). In addition to the multi-millennial tree-ring width chronologies from Torneträsk (Grudd et al., 2002), Finnish Lapland (Helama et al., 2002, 2008) and Jämtland (Gunnarson et al., 2003), several millennium-long tree-ring datasets were produced within the EU funded "Millenniu" project (McCarroll et al., 2013). Due to the superior performances of maximum latewood density (MXD, e.g., Briffa et al., 2002), and the recently developed ΔDensity method (Björklund et al., 2014a, 2015), as warm-season temperature indicators, it has been shown that these proxies are to be preferred when high-resolution reconstructions of Late-Holocene temperatures are targeted. In Fennoscandia, most sampling for millennium-long temperature reconstructions have been focused to regions close to the latitudinal tree limit (Esper et al., 2012; McCarroll et al., 2013; Melvin et al., 2013). However, to represent the whole of Fennoscandia with more fidelity, data from more southerly locations are also needed (Linderholm et al., 2015). Indeed, a few studies have produced long reconstructions from more southerly sites. Helama et al. (2014) reconstructed May–September temperature variability in southern Finland (around 61° N) for the last millennium using MXD data. In Sweden, MXD from Jämtland (63° N; (Gunnarson et al., 2011); henceforth G11, referring to the temperature reconstruction), minimum blue intensity from Mora (61° N; (Graham et al., 2011)) and adjusted Δblue intensity from Jämtland and Arjeplog (63° N and 65° N; (Björklund et al., 2015)) have been used to infer past warm-season temperatures, but these reconstructions only cover the last 800–900 years. Previously, Linderholm and Gunnarson (2005) used tree-ring width data to reconstruct June–August mean temperature for the last 3600 years in central Scandinavia. However, the tree-ring width data could only explain 39 % of the observed temperature variance during 1861–1946, and the data had a gap between 887 CE and 907 CE.

The primary aim of this study was to extend G11 back in time to cover the MCA. Moreover, G11 contained data collected from historical buildings in west-central Sweden, which were sampled in the late 1980s as a part of an archaeological survey by Kvartärbiologiska Laboratoriet in Lund, Sweden. The historical samples, covering the period between 1107 CE and 1827 CE with a gap during 1292–1315 CE, were combined with samples from living trees and snags (remains of dead trees) collected in the mountains in the early 2000s, yielding a reconstruction spanning 1107–2006 CE. The geographical origins of some of the historical samples in G11 are unclear, but they likely came from lowland locations, about 300 meters below the present tree-line, and should thus not be optimal as the backbone of a temperature reconstruction (Fritts , 1976). Therefore, we also aimed at, as far as possible, replacing the historical samples with samples collected from past and present tree-line environments where the provenance of the trees was known. Using this new reconstruction, we re-examined the warm-season temperature evolution in central Scandinavia during the last 1150 years, and compared it to other reconstructions from northern and eastern Fennoscandia (Melvin et al., 2013; Esper et al., 2012; Helama et al., 2014). This improved dataset allows us to provide new insight into temperature variability during the last millennium in central Scandinavia.

This paper is organized as follows: the tree-ring and meteorological data as well as reconstruction methods are presented in section 2; Section 3 presents and discusses the new central Scandinavian temperature reconstruction, and compares it with other millennium-long Fennoscandian temperature reconstructions; Conclusions are given in Section 4.

2 Data and method

2.1 Study area

The study area is located in the province of Jämtland, east of the main divide of the Scandinavian Mountains in west-central Sweden. Due to the geographical setting, there is a distinct climate gradient in the region (Linderholm et al., 2003). East of the Scandinavian Mountains, climate can be described as semi-continental. However, the proximity to the Norwegian Sea, lack of high mountains in the west, and the eastwest oriented valleys allow moist air to be advected from the ocean, providing an oceanic influence to the area (Johannessen , 1970; Johansson and Chen , 2003; Bojariu and Giorgi , 2005). Consequently, the study area is a border zone between oceanic and continental climates (Wallén , 1970). On short timescales, the climate of this area is influenced by the North Atlantic Oscillation (NAO) (Chen and Hellström , 1999; Busuioc et al., 2001; Folland et al., 2009), while it is affected by North Atlantic sea-surface temperature (SST) on longer timescales (Rodwell et al., 1999; Rodwell and Folland , 2002). The elevation of this area ranges from 800 to 1000 m a.s.l., and scattered alpine massifs to the south reach approximately 1700 m a.s.l.. Glacial deposits dominate the area, mainly till but also glaciofluvial deposits, peatlands and small areas of lacustrine sediments (Lundqvist , 1969). *Pinus sylvestris* L. (Scots pine), *Picea abies* (L.) H. Karst. (Norway

spruce) and *Betula pubescens* Ehrh. (Mountain birch) are the main tree species in central Scandinavian Mountains. Although large-scale forestry operations have been carried out in some parts of the region, the human impacts on trees growing close to the tree line is limited (Gunnarson et al., 2012). Due to the short and cool summers, snags can be preserved for more than 1000 years on the ground (Linderholm et al., 2014) and the subfossil wood can be preserved for hundreds to thousands of years in the sediments of small mountain lakes (Gunnarson , 2008).

2.2 Description of the tree-ring data

Scots pine tree-ring samples, collected from seven sites in the central Scandinavian Mountains and from historical buildings east of the mountains, were used in the new temperature reconstruction. Fig. 1 shows the locations of the sampling sites. All the sites except for the historical-building samples are located within 20 km of each other, covering an altitudinal gradient of 200 m with slightly different moisture-environments ranging from relatively well drained soils to wetter lake-shore conditions. The historical-building samples used in this study were collected from buildings in the southeast of Jämtland. Altogether, 99 samples from both living trees and snags were collected from Mount Furuberget at an elevation of ca. 650 m a.s.l.. The sampling sites were characterized by open pine forests with limited competitions between the trees. The sampling sites had thick vegetation layers with woody dwarf shrubs and mosses. Out of the 99 samples, 35 were previously used in the G11 reconstruction. An additional 40 samples, mainly from snags, were collected from the nearby Mount Håckervalen, on elevations ranging from 650 m a.s.l. (present-day tree line in the area) up to 800 m a.s.l. (Linderholm et al., 2014). 32 samples from subfossil wood collected from the small mountain lakes of Lill-Rörtjärnen, Östra Helgtjärnen and Jens-Perstjärnen, at 560, 646 and 700 m a.s.l. respectively (Gunnarson , 2008), were also included. The historical samples from Bodsjö, which made up the older part of G11, was downloaded from the International Tree-Ring Data Bank (ITRDB). The MXD values of the historical samples have been previously obtained using DENDRO2003 X-ray instrumentation from Walesch Electronic (www.walesch.ch). Table 1 provides a full description of the sampling sites and tree-ring data.

The new MXD samples were measured at the tree-ring laboratory of Stockholm University using the ITRAX wood scanner from Cox Analytical Systems (http://www.coxsys.se). Thin laths (1.20 mm thick) were cut from each sample using a twin-bladed circular saw, and subsequently put in a Soxhlet apparatus with pure alcohol to remove resins and other compounds. After being processed in the Soxhlet for at least 24 hours, the laths were acclimatized in a room with controlled temperature and humidity to have ca. 12 % water content, and then mounted in a sample holder. The samples were exposed to a narrow, high energy, X-ray beam. The chrome tube in the ITRAX was tuned to 30 kV and 50 mA, with 75 ms step time. The opening time of the sensor slit was set to 20 µm at each step. From the sensor, a 16-bit, greyscale, digital image with a resolution of 1270 dpi was produced. The grey levels of the image were calibrated to values of wood density using a cellu-

lose acetate calibration wedge provided by Walesch Electronics. The MXD data was obtained using the image processing software WinDENDRO.

Zhang et al. (2015) found that MXD data from the study area covering the same time period but originating from different elevations/sites can have systematic differences in terms of mean values. Because the older snag samples in this study were found at progressively higher elevations, as well as contrasting growth environments, serious biases could thus be introduced into an average chronology based on all data, both in terms of the annual to decadal variability, but perhaps even more so in the longer-term trends, if the differences in absolute MXD values caused by elevation and local moisture conditions are not accounted for (Zhang et al., 2015). Therefore, we adjusted the mean MXD values from trees growing at different elevations as well as the subfossil samples, representing a wetter growth environment than the tree-line trees, to have the same mean during a common period. Following the protocol proposed by Zhang et al. (2015), we used the mean MXD values of the samples from Furuberget-north for the period 1300–1550 CE as the reference to correct the data (see Table 1 for adjustment values for each site). The Furuberget-north data was chosen as reference because it had the highest sample replication and widest temporal coverage.

In a tree-ring MXD series, MXD values change with age. Therefore, when applying the mean-adjustment methodology (Zhang et al., 2015) this should be taken into consideration, and each group of samples should have a homogeneous age distribution in the selected reference period, as well as the adjustment periods. The time-spans of the adjusted and reference samples are shown in Fig. A.1. To further validate the mean-adjustment of this data material, Fig. A.2 shows the age-aligned average curves for the samples partly or fully covering the reference periods before and after the mean-adjustment, along with the average curve of the reference samples. The average curves were smoothed using spline functions. The smoothed average curves show that MXD values generally decrease with tree's age. The average curve of the adjusted samples displays the same mean MXD level as the average curve of the reference samples. This result indicates that the distribution of ages is not the main reason why the mean-values of the samples in different groups/sites are different in the reference period. The samples from Furuberget-south and Håckervalen-north were not adjusted, because both groups of samples were collected from sites where growing conditions (open forests on relatively well drained soils) and elevations were similar to the reference samples.

2.3 Standardisation methods

If tree-ring data is going to be used to attain high-quality climate information, it is necessary to remove as much non-climatic "noise" as possible before building a chronology from the individual tree-ring series (Fritts , 1976). The non-climatological growth expression is usually represented with a least square fitted negative exponential function, polynomial or spline

This limitation can be overcome by quantifying the non-climatological growth expression for an entire population as an average of the growth of all samples aligned by cambial age, which then can

be represented by a single mathematical function. Subsequently this function is removed from each individual tree-ring measurement, an approach called Regional Curve Standardisation (RCS, Briffa et al., 1992). However, by using one single function for all tree-ring series, mid-frequency variability may be removed in the attempt to preserve the low-frequency (>segment length) variability (Melvin , 2004), along with possible trend distortion as described in (Melvin and Briffa , 2008, 2014a, b). Melvin and Briffa (2014a, b) showed that using multi-curve RCS can, however, efficiently remove these biases. Alternatively, the non-climatological expression in tree-ring data can be quantified with an individual signal-free (SF) approach, described in Melvin and Briffa (2008), but this approach is also limited in the lower-most frequencies (Björklund et al., 2013).

However, by using the SF individual fitting approach and at the same time letting the derived functions to have a similar mean as their respective cambial age segment of the regional curve (RC) before subtraction into indices, stand competition etc. can also be addressed without losing the long timescale component (Björklund et al., 2013). This method is a hybrid of the RCS and individual SF standardization, and was termed RSFi. In this study, we produced MXD chronologies using two standardisation methods: two-curve signal-free RCS (fitted by age-dependent splines) and RSFi (fitted by age-dependent splines), where the RSFi chronology was used for the new reconstruction. In both methods, residuals between raw data and fitted functions were calculated, and subsequently averaged to produce the final chronology. The standardisations were performed using the software RCSsigFree (Cook et al., 2014) and CRUST (Melvin and Briffa , 2014a, b). The expressed population signal (EPS) criterion was used to evaluate the robustness of the chronology. An EPS value represents the percentage of the variance in the hypothetical population signal in the region that is accounted for by the chronology, where EPS values greater than 0.85 are generally regarded as sufficient (Wigley et al., 1984). Here the EPS values were calculated in a 50–year window with a 1–year lag.

2.4 Instrumental data

Monthly temperature data from the closest meteorological station, Duved (400 $\mathrm{m\,a.s.l.}$, 63.38° N, 12.93° E), was used to assess the temperature signal reflected by the chronology. Since the data from this station only cover the period 1911–1979, the data was extended back to 1890 CE and up to 2011 CE using linear regression on monthly temperature data from an adjacent station: Östersund (376 $\mathrm{m\,a.s.l.}$, 63.20° N, 14.49° E. Data from Östersund explained on average 91.5 % of the interannual variance of Duved monthly temperature (based on the overlapping period 1911–1979). The temperature data from Östersund came from two sources: the Nordklim dataset (1890–2001) (Tuomenvirta et al., 2001), and Swedish Meteorological and Hydrological Institute (SMHI, 2001–2011 CE). The locations of Duved and Östersund stations are shown in Fig. 1.

2.5 Climate signal and reconstruction technique

We calculated correlations between the new MXD chronology and instrumental monthly mean temperatures from Duved over the period 1890–2011 CE. Fig. 3 shows that it is significantly correlated ($p < 0.01$) with all individual months from April to September, and the correlation with mean April–September temperature is 0.77 (0.81 ($p < 0.01$) if only interannual variability were considered). Same results were obtained (0.77, $p < 0.01$) when correlating the MXD chronology with mean April–September temperature from the closest grid in the CRU TS3.23 $0.5^\circ \times 0.5^\circ$ dataset (Harris et al., 2014) over the period 1901–2011. A transfer model was developed using simple linear regression, where the April–September temperature anomalies (deviations from the 1961–1990 mean) were set as the predictand and the MXD data of the current year (t), as the predictor. The temporal stability of the model was tested with a split sample calibration/verification procedure

The final model was calibrated over the full 1890–2011 period. The uncertainty of the reconstruction was estimated from two sources: chronology characteristics (temporal variations in replication) and the calibration statistics according to the methods of Yang et al. (2014). The uncertainty in the chronology was estimated by $+/-$ 2 times the standard error (i.e. the standard deviation of all MXD index values in each year divided by the square root of the sample replication). The calibration uncertainty was estimated from the standard deviation of the reconstruction residuals (i.e. the difference between observed and reconstructed temperatures). The error of the reconstruction was estimated by the square root of the sum of the squared chronology error and the squared calibration uncertainty. The uncertainty of the reconstruction was then estimated by $+/-$ 2 times of the reconstruction error.

3 Result and discussion

3.1 The new reconstruction and reconstruction statistics

The calibration and verification statistics are summarized in Table 2. The RE and CE statistics are well above zero, and thus pass the validation tests (National Research Council , 2006). Fig. 4a shows a linear relationship between the MXD data and Duved April–September mean temperatures over the period 1890–2011. The reconstructed and observed warm-season temperatures show good agreement on interannual and multidecadal timescales (Fig. 4b). The reconstruction has a slightly smaller spatial representation than observed station data when compared to gridded temperatures (Fig. 5). However, the new reconstruction still represents much of central Fennoscandia, and has a much more southerly expression than the northern MXD chronologies mentioned in the introduction (Melvin et al., 2013; Esper et al., 2012; McCarroll et al., 2013), and more western expression than Helama et al. (2014).

3.2 Central Scandinavian warm-season temperature evolution

Fig. 6a shows that the differences between the mean-adjusted and the non-adjusted MXD chronologies mainly occur before 1300 CE. The mean-adjusted chronology shows lower values between 1150 and 1300 and higher values between 850 and 1100 compared to the non-adjusted chronology. Clearly not using the mean adjustment would have large impacts on the interpretation of the temperature evolution during the last millennium. If possible this principle should always be utilized when data from slightly different growth environments, with sufficient overlap, are composited, before standardization. Fig. 6c shows that the EPS values are above 0.85 during most of the last millennium, testifying to the robustness of the chronology in representing the hypothetical population signal. However, there is a dip in EPS values during the period 1150–1200 which reduces the validity of the reconstruction in this period. EPS values are influenced by two factors: number of samples and inter-series correlations (Wigley et al., 1984). Obviously, the dip in EPS values in this case should be attributed to relatively weak inter-series correlation over that time period compared to other time periods during the last millennium. It should be noted that the chronology during this period consist of both tree-line and low-elevation (historical) samples. However, during most of the last millennium, the variability of the tree-ring samples from the two sources (tree-line and historical) does not show obvious differences at interannual (not show) to centennial (Fig. 7) timescales. Therefore, to find out the reason for the low inter-series correlation more in situ samples from that period are needed.

When comparing the MXD chronologies based on the RSFi and the two-curve signal-free RCS standardisation (Fig. 6b), the two chronologies are rather similar. Because of this, and the assumption that the former methodology has a greater chance at removing mid-frequency noise (Björklund , 2014b), we chose the RSFi method for our reconstruction. Fig. 6d shows the reconstructed warm-season temperature in central Scandinavia, henceforth referred to as C-Scan, during the past 1150 years. C-Scan displays a cooling trend over the period 850–1900, followed by a sharp temperature increase in the 20th century. C-Scan suggests a moderate MCA warm-peak during ca. 1000 CE to 1100 CE in central Scandinavia. Improved understanding of spatiotemporal characteristics of MCA is important in terms of understanding the dynamic origin of MCA. Proxy-based spatial annual temperature reconstructions have delineated a strong and persistent $La Niña$-like climate pattern globally during MCA. The spatial pattern of the reconstructed temperature changes (MCA-LIA) imply that MCA may be caused by dynamical responses to natural radiative forcing (Mann et al., 2009). However, climate model simulations (as shown in González-Rouco et al., 2011) with strong solar forcings failed to reproduce such a spatial pattern (in Mann et al., 2009). In contrast, the climate model with reduced solar forcing, allowing for internal variability to be more prominent, show less uniform temperature responses in sign as those of the reconstructed global annual temperature changes (in Mann et al., 2009). Therefore, internal variability of climate system as a possible reason of the MCA-LIA anomalies has been suggested (González-Rouco et al., 2011). Recently, Goosse et al. (2012) simulated MCA-LIA transition using data assimilation method, and indicated

spatial pattern of temperature during MCA could be caused by weak radiative forcing combined with a modification of atmospheric circulations, and the changes of the atmospheric circulations could be related to either climate-system internal dynamics or dynamical responses to weak changes of radiative forcing. We can see that reconstructions of surface temperature pattern provide possibilities for all these attribution studies. Therefore, high-quality temperature reconstructions in regional and sub-regional scale are still needed. Our reconstruction indicates that the warm-season warmth during MCA is not so pronounced in central Scandinavia, which improves our knowledge about spatial pattern of surface air temperature on global and regional timescales. The new reconstruction will also add values to existing regional temperature reconstructions (e.g. Luterbacher et al., 2016).

C-Scan also indicates that in this region the cold period known as the Little Ice Age (LIA, Grove , 2001) spanned the mid-16th century to the end of the 19th century, where the coldest 100–year period was found in the late 18th to late 19th century. Both the coldest 10- and 30-year periods were found around 1600 CE. The warmest 10, 30 and 100-year periods during the last millennium were all found in the 20th century. Comparing the MCA to the 20th century, the warmest 10- and 30- and 100-year in the 20th century are 0.3°C, 0.1°C and 0.03°C warmer in the 20th century than those in the 10th and 13th centuries respectively.

Fig. 7 shows a comparison between C-Scan and G11. The two reconstructions show coherent variability at multidecadal to centennial timescales during the period 1300–2000. However, the 12th century is portrayed as much warmer in G11 than in C-Scan, and we largely attribute this discrepancy to the omission of adjusting the mean values of the samples from different elevations in G11. However, if this feature is disregarded, the comparison between C-Scan and G11 actually show that the historical-building samples perform quite well in representing the temperature variability at multidecadal to centennial timescales. Considering the performance of the historical samples and the temporarily low replication of the newly collected samples around 1200 CE, we argue that it is better to use the historical samples when sample depth is low, than not to use it at all. Therefore, we included mean adjusted historical samples for the period 1107–1291 CE in our reconstruction. The EPS values are improved over that time period, but still do not reach the 0.85 threshold.

Compared to G11, the merit of C-Scan is manifested by three aspects: 1) C-Scan covers the whole of MCA and can be used to interpret the temperature evolution during this important phase in central Scandinavia. 2) The application of the mean-adjustment method. Our results suggest that also the historical-building samples, used in G11, should be separately mean-adjusted according to their origin and mean values, and not be treated as a homogenous dataset. 3) C-Scan is to 92 % based on the samples collected from a relatively small mountain area, close to the local tree line, compared to G11 that was based on 73 % historical samples. Even though the historical samples seemingly perform in a similar way as the tree-line samples, trees at the limit of their distribution should be more sensitive and thus perform better, and be preferred in a reconstruction, according to the principle of limiting factors (Fritts , 1976). This is perhaps corroborated by the fact that the new reconstruction

displays a larger variance at some periods, such as stronger cooling events around 1450 CE and 1600 CE than those in G11. This could be interpreted as a more coherent variability (lower noise level) among the newly collected samples than the historical-building samples, which is always strived for.

3.3 Comparing C-Scan with other Fennoscandian summer temperature reconstructions

As mentioned earlier, annually resolved summer and warm-season temperature reconstructions covering the entire last millennium, based on MXD data, have almost exclusively focused on northern Fennoscandia ((McCarroll et al., 2013), henceforth referred to as Mc13; (Esper et al., 2012; Melvin et al., 2013; Matskovsky and Helama , 2014), henceforth referred to as MH14), with the exception of the reconstruction for southern Finland ((Helama et al., 2014), henceforth referred to as H14). A general feature of these reconstructions is a cooling trend during the past millennium until the end of 19th century, consistent with the reduction in high-latitude summer solar insolation related to orbital forcing (Helama et al., 2010; Esper et al., 2012), followed by an abrupt warming trend during 20th century, related to increasing $CO2$ concentrations in the atmosphere (Stocker et al., 2013). However, differences among these reconstructions, even those focused on the northernmost part of the region, have been discussed, (e.g. Matskovsky and Helama , 2014; Linderholm et al., 2015). In Fig. 8, C-Scan is compared with MH14, Mc13 and H14. C-Scan shows smaller variance than other three reconstructions, because it was calibrated based on longer time-window (i.e. April–September) than the others (MH14: June–July; Mc13: June–August; H14: May–September). The multidecadal variability of H14 generally differs from the other ones, where the pronounced cooling during the LIA stands out. The other segments of the reconstructions agree quite well, although Mc13 in general shows cooler anomalies than MH14 and C-Scan. The largest discrepancy among the reconstructions is found between 900 and 1100 CE (the MCA), where MH14 shows persistent warm anomalies, whereas Mc13 shows cooling and in C-Scan temperatures are only slightly above the long-term average. MCA temperatures in H14 are similar to C-Scan, but slightly higher.

June–August mean temperature variability are rather coherent with April–September mean temperature variability at different timescales in Scandinavia (not shown), so different calibration time-windows are not likely the reason why the four reconstructions show differences in their variability. It is possible that at least part of the discrepancies among the reconstructions can be attributed to methodological issues, such as changes in numbers of samples through time in the chronologies, or periods where trees show less coherent growth patterns (e.g. the 1150–1200 period in C-Scan). Such issues can be alleviated through careful selection of the tree-ring data and more coherent standardisation method and parameters (Frank et al., 2010; Björklund , 2014b). However, the differences in reconstructed temperatures may also be expressions of sub-regional differences associated with varying atmospheric circulations patterns influence across Fennoscandia through time. Linderholm et al. (2015) discussed the possibility that changes in the average positions of circulation patterns

such as the NAO, related to changes in the polar jet stream configuration, could have an influence on the homogenous summer temperature pattern in Fennoscandia observed today. Likely, due to the proximity of the study region to the ocean, the influence of e.g. the Atlantic Multidecadal Oscillation can also be of importance. Furthermore, Irannezhad et al. (2014) found that the trends of observed annual and seasonal surface air temperature show spatial differences in Finland, and that the warm-season temperature can be related to different regional-scale circulation patterns such as the East Atlantic, West Russia, Scandinavian and West Pacific patterns in different sub-region. Thus, it is likely that summer temperature variability in different sub-regions throughout Fennoscandia are controlled by different circulation patterns, and that asymmetric changes of these circulation patterns induce spatial differences in summer temperature evolution. A more detailed study of regional temperature patterns, and their associated regional-scale circulation patterns, in Fennoscandia can be useful to test if the spatial differences of warm-season temperature evolution occur in the past during different climate settings, especially during the MCA, being partly an analogue to the present warming.

4 Conclusions

In this study we successfully updated and extended the MXD data previously used to reconstruct central Scandinavian warm-season temperatures. The new reconstruction, C-Scan, now extends back to 850 CE including also the MCA. Compared to the previous reconstruction, G11, in C-Scan the issue of biases arising from samples from different locations was appropriately addressed and corrected using the mean-adjustment method, and C-Scan is largely based on high-quality tree-line samples collected from a smaller area.

C-Scan suggests a moderate MCA warm-peak during ca. 1000 CE to 1100 CE in central Scandinavia and a LIA lasting from the mid-16th century to the end of the 19th century. During the last millennium, the late 18th century to late 19th century was the coldest 100-year period in central Scandinavia, where the coldest 10- and 30-year periods occurred around 1600 CE. The warmest 10-, 30- and 100-year periods were found in 20th century. C-Scan indicates lower temperature during the late MCA (ca. 1130–1210 CE) and higher temperature during the LIA (1610–1850 CE) than G11.

Some differences in multidecadal to multicentennial variability between C-Scan and other MXD-based temperature reconstructions from Fennoscandia were found, suggesting regional differences of summer/warm-season temperature evolution, possibly linked to varying influences of atmospheric circulation patterns. However, this needs to be further investigated.

Acknowledgements. We acknowledge the County Administrative Boards of Jämtland for giving permissions to conduct dendrochronological sampling, and Mauricio Fuentes, Petter Stridbeck, Riikka Salo, Emad Farahat, Kristina Seftigen, Eva Rocha and Peter Seftigen for their help in the field. We also thank Laura McGlynn and Håkan Grudd for assistance in the MXD measurements and Andrea Seim for helping out with GIS and correcting the manuscript. This work was supported by Grants from the two Swedish research councils (Vetenskapsrådet and Formas, Grants to Hans Linderholm) and the Royal Swedish Academy of Sciences (Kungl. Vetenskapsakademien) (grant to Peng Zhang). This research contributes to the strategic research areas Modelling the Regional and Global Earth system (MERGE), and Biodiversity and Ecosystem services in a Changing Climate (BECC) and to the PAGES2K initiative. This is contribution # 33 from the Sino-Swedish Centre for Tree-Ring Research (SISTRR).

References

Bindoff, N. L., Stott, P. A., AchutaRao, K. M., Allen, M. R., Gillett, N., Gutzler, D., Hansingo, K., Hegerl, G., Hu, Y., Jain, S., Mokhov, I. I., Overland, J., Perlwitz, J., Sebbari, R., and Zhang, X.: Detection and Attribution of Climate Change: from Global to Regional. In: Climate Change 2013: The Physical Science Basis. Contribution of Working Group I to the Fifth Assessment Report of the Intergovernmental Panel on Climate Change [Stocker, T. F., Qin, D., Plattner, G. K., Tignor, M., Allen, S. K., Boschung, J., Nauels, A., Xia, Y., Bex, V., and Midgley, P. M.(eds.)], Cambridge University Press, Cambridge, United Kingdom and New York, NY, USA, 2013.

Björklund, J. A., Gunnarson, B. E., Krusic, P. J., Grudd, H., Josefsson, T., Östlund, L., and Linderholm, H. W.: Advances towards improved low-frequency tree-ring reconstructions, using an updated Pinus sylvestris L. MXD network from the Scandinavian Mountains, Theor. Appl. Climatol., 113, 697–710, 2013.

Björklund, J. A., Gunnarson, B. E., Seftigen, K., Esper, J., Linderholm, H. W.: Blue intensity and density from Northern Fennoscandian tree rings: using earlywood information to improve reconstructions of summer temperature. Climate of the Past, 10, 877–885, 2014a.

Björklund, J. A.: Tree-rings and climate: standardization, proxy development, and Scandinavian summer temperature history, PhD thesis, Department of Earth Sciences, University of Gothenburg, Sweden, 2014b.

Björklund, J., Gunnarson, B. E., Seftigen, K., Zhang, P., and Linderholm, H. W.: Using adjusted Blue Intensity data to attain high-quality summer temperature information: A case study from Central Scandinavia, The Holocene, 25(3), 547–556, 2015.

Bojariu, R., and Giorgi, F.: The North Atlantic Oscillation signal in a regional climate simulation for the European region, Tellus A, 57(4), 641–653, 2005.

Briffa, K. R., Jones, P. D., Bartholin, T. S., Eckstein, D., Schweingruber, F. H., Karlén, W., Zetterberg, P., and Eronen, M.: Fennoscandian summers from AD 500: temperature changes on short and long timescales, Climate Dynamics, 7, 111–119, 1992.

Briffa, K. R., Jones, P. D., Schweingruber, F. H., Karlén, W., and Shiyatov, S. G.: Tree-ring variables as proxy-climate indicators: problems with low-frequency signals, Springer, 9–41, 1996.

Briffa, K. R., Osborn, T. J., Schweingruber, F. H., Harris, I. C., Jones, P. D., Shiyatov, S. G., and Vaganov, E. A.: Lowfrequency temperature variations from a northern tree ring density network. Journal of Geophysical Research: Atmospheres (19842012), 106(D3), 2929–2941, 2001.

Briffa, K. R., Osborn, T. J., Schweingruber, F. H., Jones, P. D., Shiyatov, S. G., and Vaganov, E. A.: Tree-ring width and density data around the Northern Hemisphere: Part 1, local and regional climate signals, The Holocene, 12, 737–757, 2002.

Busuioc, A., Chen, D., Hellström, C.: Temporal and spatial variability of precipitation in Sweden and its link with the large scale atmospheric circulation, Tellus, 53A, 348–367, 2001.

Chen, D., and Hellström, C.: The influence of the North Atlantic Oscillation on the regional temperature variability in Sweden: spatial and temporal variations, Tellus A, 51, 505–516, 1999.

Cook, E. R., and Peters, K.: The Smoothing Spline: A New Approach to Standardizing Forest Interior Tree-Ring width Series for Dendroclimatic Studies, Tree-Ring Bulletin, 41, 45–53, 1981.

Cook, E. R., Briffa, K. R., Meko, D. M., Graybill, D. A., and Funkhouser, G.: The "segment length curse" in long tree-ring chronology development for palaeoclimatic studies, The Holocene, 5, 229–237, 1995.

Cook, E. R., Krusic, P. J., and Melvin, T.: Program RCSsigFree: Version 45_v2b. Lamont-Doherty Earth Obs. Columbia University, 2014.

Esper, J., Frank, D. C., Timonen, M., Zorita, E., Wilson, R. J., Luterbacher, J., Holzkämper, S., Fischer, N., Wagner, S., and Nievergelt, D.: Orbital forcing of tree-ring data, Nature Climate Change, 2, 862–866, 2012.

Folland, C. K., Knight, J., Linderholm, H. W., Fereday, D., Ineson, S., and Hurrell, J. W.: The summer North Atlantic Oscillation: past, present, and future. Journal of Climate, 22(5), 1082–1103, 2009.

Frank, D., Esper, J., Zorita, E., and Wilson, R.: A noodle, hockey stick, and spaghetti plate: a perspective on highresolution paleoclimatology. Wiley Interdisciplinary Reviews: Climate Change, 1(4), 507–516, 2010.

Fritts, H.: Tree Rings and Climate, ACADEMIC PRESS INC. (LONDON) LTD, London, UK, 1976.

George, S. S.: An overview of tree-ring width records across the Northern Hemisphere, Quaternary Science Reviews, 95, 132–150, 2014.

González-Rouco, J. F., Fernández-Donado, L., Raible, C. C., Barriopedro, D., Lutherbacher, J., Jungclaus, J. H., Swingedouw, D., Servonnat, J., Zorita, E., Wagner, S., and Ammann, M.: Medieval Climate Anomaly to Little Ice Age transition as simulated by current climate models, PAGES News, 19(1), 7-8, 2011.

Goosse, H., Crespin, E., Dubinkina, S., Loutre, M. F., Mann, M. E., Renssen, H., Sallaz-Damaz, Y., and Shindell, D.: The role of forcing and internal dynamics in explaining the "Medieval Climate Anomaly", Climate dynamics, 39(12), 2847–2866, 2012.

Gordon, G.: Verification of dendroclimatic reconstructions. In Climate from tree rings, Hughes, M. K., Kelly, P. M., Pilcher, J. R., LaMarche, V. C., Pilcher, J. R.(eds), Cambridge University Press, Cambridge, 58–61, 1982.

Graham, R., Robertson, I., McCarroll, D., Loader, N., Grudd, H., and Gunnarson, B.: Blue Intensity in Pinus sylvestris: application, validation and climatic sensitivity of a new palaeoclimate proxy for tree ring research, in: AGU Fall Meeting Abstracts, 1, 9–41, 2011.

Grove, J. M.: The Initiation of the "Little Ice Age" in Regions Round the North Atlantic, in: The Iceberg in the Mist: Northern Research in pursuit of a "Little Ice Age", Springer, 53–82, 2001.

Grove, J. M., and Switsur, R.: Glacial geological evidence for the Medieval Warm Period, Climatic Change, 26, 143–169, 1994.

Grudd, H., Briffa, K. R., Karlén, W., Bartholin, T. S., Jones, P. D., and Kromer, B.: A 7400-year tree-ring chronology in northern Swedish Lapland: natural climatic variability expressed on annual to millennial timescales, The Holocene, 12, 657–665, 2002.

Gunnarson, B. E.: Temporal distribution pattern of subfossil pines in central Sweden: perspective on Holocene humidity fluctuations, The Holocene, 18(4), 569–577, 2008.

Gunnarson, B. E., Borgmark, A., and Wastegård, S.: Holocene humidity fluctuations in Sweden inferred from dendrochronology and peat stratigraphy, Boreas, 32, 347–360, 2003.

Gunnarson, B. E., Linderholm, H. W., and Moberg, A.: Improving a tree-ring reconstruction from west-central Scandinavia: 900 years of warm-season temperatures, Climate Dynamics, 36(1–2), 97–108, 2011.

Gunnarson, B. E., Josefsson, T., Linderholm, H. W., and Östlund, L.: Legacies of pre-industrial land use can bias modern tree-ring climate calibrations, Clim. Res., 53, 63–76, 2012.

Harris, I., Jones, P., Osborn, T., and Lister, D.: Updated high resolution grids of monthly climatic observations – the CRU TS3.10 Dataset, International Journal Climatology, 34(3), 623–642, 2014.

Helama, S., Lindholm, M., Timonen, M., Meriläinen, J., and Eronen, M.: The supra-long Scots pine tree-ring record for Finnish Lapland: Part 2, interannual to centennial variability in summer temperatures for 7500 years, The Holocene, 12, 681–687, 2002.

Helama, S., Mielikäinen, K., Timonen, M., and Eronen, M.: Finnish supra-long tree-ring chronology extended to 5634 BC. Norwegian Journal of Geography, 62(4), 271–277, 2008.

Helama, S., Fauria, M. M., Mielikäinen, K., Timonen, M., and Eronen, M.: Sub-Milankovitch solar forcing of past climates: mid and late Holocene perspectives, Geological Society of America Bulletin, 122(11-12), 2010.

Helama, S., Vartiainen, M., Holopainen, J., Mäkelä, H. M., Kolström, T., and Meriläinen, J.: A palaeotemperature record for the Finnish Lakeland based on microdensitometric variations in tree rings, Geochronometria, 41, 265–277, 2014.

Irannezhad, M., Chen, D., and Kløve, B.: Interannual variations and trends in surface air temperature in Finland in relation to atmospheric circulation patterns, 19612011, International Journal of Climatology, 35(10), 3078–3092, 2014.

Johannessen, T. W.: The climate of Scandinavia, Climates of Northern and Western Europe, World survey of climatology, 5, 23–80, 1970.

Johansson, B. and Chen, D.: The influence of wind and topography on precipitation distribution in Sweden: Statistical analysis and modelling, International Journal of Climatology, 23(12), 1523–1535, 2003.

Lamb, H. H.: Climatic fluctuations. World survey of climatology, 2, 173–249, 1969.

Linderholm, H. W., Solberg, B. Ø., and Lindholm, M.: Tree-ring records from central Fennoscandia: the relationship between tree growth and climate along a westeast transect, The Holocene, 13(6), 887–895, 2003.

Linderholm, H. W., and Gunnarson, B. E.: Summer temperature variability in central Scandinavia during the last 3600 years, Geografiska Annaler: Series A, Physical Geography, 87(1), 231–241, 2005.

Linderholm, H. W., Björklund, J. A., Seftigen, K., Gunnarson, B. E., Grudd, H., Jeong, J. H., Drobyshev, I., and Liu, Y.: Dendroclimatology in Fennoscandia – from past accomplishments to future potential, Climate of the Past, 6, 93–114, 2010.

Linderholm, H. W., Zhang, P., Gunnarson, B. E., Björklund, J., Farahat, E., Fuentes, M., Rocha, E., Salo, R., Seftigen, K., and Stridbeck, P.: Growth dynamics of tree-line and lake-shore Scots pine (Pinus sylvestris L.) in the central Scandinavian Mountains during the Medieval Climate Anomaly and the early Little Ice Age, Paleoecology, 2, 20, doi:10.3389/fevo.2014.00020, 2014.

Linderholm, H., Björklund, J., Seftigen, K., Gunnarson, B., and Fuentes, M.: Fennoscandia revisited: a spatially improved tree-ring reconstruction of summer temperatures for the last 900 years, Climate Dynamics, 45, 933–947, 2015.

Lundqvist, J.: Beskrivning till jordartskarta över Jämtlands län: 4 Karten. Kt, Sveriges Geologiska Undersökning, 1969.

Luterbacher, J., Werner, J. P., Smerdon, J. E., Fernndez-Donado, L., González-Rouco, F. J., Barriopedro, D., Ljungqvist, F. C., Büntgen, U., Zorita, E., Wagner, S., Esper, J., McCarroll, D., Toreti, A., Frank, D., Jungclaus, J. H., Barriendos, M., Bertolin, C., Bothe, O., Brázdil, R., Camuffo, D., Dobrovolný, P., Gagen, M., García-Bustamante, E., Ge, Q., Gómez-Navarro, J. J., Guiot, J., Hao, Z., Hegerl, G. C., Holmgren, K., Klimenko, V. V., Martín-Chivelet, J., Pfister, C., Roberts, N., Schindler, A., Schurer, A., Solomina, O.,

von Gunten, L., Wahl, E., Wanner, H., Wetter, O., Xoplaki, E., Yuan, N., Zanchettin, D., Zhang, H., and Zerefos, C.: European summer temperatures since Roman times, Environmental Research Letters, 11(2), doi:10.1088/1748-9326/11/2/024001, 2016.

Mann, M. E., Zhang, Z., Rutherford, S., Bradley, R. S., Hughes, M. K., Shindell, D., Ammann, C., Faluvegi, G., and Ni, F.: Global signatures and dynamical origins of the Little Ice Age and Medieval Climate Anomaly, Science, 326(5957), 1256–1260, 2009.

Matskovsky, V. V., and Helama, S.: Testing long-term summer temperature reconstruction based on maximum density chronologies obtained by reanalysis of tree-ring data sets from northernmost Sweden and Finland, Climate of the Past, 10(4), 1473–1487, 2014.

McCarroll, D., Loader, N. J., Jalkanen, R., Gagen, M. H., Grudd, H., Gunnarson, B. E., Kirchhefer, A. J., Friedrich, M., Linderholm, H. W., and Lindholm, M.: A 1200-year multiproxy record of tree growth and summer temperature at the northern pine forest limit of Europe, The Holocene, 23(4), 471–484, 2013.

Melvin, T. M.: Historical Growth Rates and Changing Climatic Sensitivity of Boreal Conifers, PhD Thesis, Climatic Research Unit, University of East Anglia, Norwich, UK, 2004.

Melvin, T. M., and Briffa, K. R.: A "signal-free" approach to dendroclimatic standardisation, Dendrochronologia, 26, 71–86, 2008.

Melvin, T. M., Grudd, H., and Briffa, K. R.: Potential bias in "updating" tree-ring chronologies using regional curve standardisation: re-processing 1500 years of Torneträsk density and ring-width data, The Holocene, 23, 364–373, 2013.

Melvin, T. M., Briffa, K. R.: CRUST: Software for the implementation of regional chronology standardisation: part 1. Signal-free RCS, Dendrochronologia, 32(1), 7–20, 2014a.

Melvin, T. M., Briffa, K. R.: CRUST: Software for the implementation of Regional Chronology Standardisation: Part 2. Further RCS options and recommendations, Dendrochronologia, 32(4), 343–356, 2014b.

National Research Council: Surface Temperature Reconstructions for the Last 2000 Years. The National Academies Press: Washington, DC, 160 pp, 2006.

van Oldenborgh, G. J., Drijfhout, S., van Ulden, A., Haarsma, R., Sterl, A., Severijns, C., Hazeleger, W., and Dijkstra, H.: Western Europe is warming much faster than expected, Clim. Past, 5, 1–12, 2009.

PAGES 2k Consortium: Continental-scale temperature variability during the last two millennia, Nature Geoscience, 6, 339–346, 2013.

Rodwell, M., and Folland, C.: Atlantic air–sea interaction and seasonal predictability, Quarterly Journal of the Royal Meteorological Society, 128(583), 1413–1443, 2002.

Rodwell, M., Rowell, D., and Folland, C.: Oceanic forcing of the wintertime North Atlantic Oscillation and European climate, Nature, 398(6725), 320–323, 1999.

Stocker, T., Qin, D., Plattner, G., Tignor, M., Allen, S., Boschung, J., Nauels, A., Xia, Y., Bex, V., and Midgley, P.: IPCC, 2013: summary for policymakers, in: Climate Change 2013: The Physical Science Basis, Contribution of Working Group I to the Fifth Assessment Report of the Intergovernmental Panel on Climate Change, Cambridge Univ. Press, Cambridge, UK, 3–29, 2013.

Tuomenvirta, H., Drebs, A., Førland, E., Tveito, O. E., Alexandersson, H., Laursen, E. V., and Jónsson, T.: Nordklim data set 1.0 description and illustrations, Tech. rep., DNMI Report, 27, 2001.

Wallén, C. C. (ed.) Climates of Northern and Western Europe, Elsevier, Amsterdam, 1970.

Wigley, T. M., Briffa, K. R., and Jones, P. D.: On the average value of correlated time series, with applications in dendroclimatology and hydrometeorology, Journal of Climate and Applied Meteorology, 23(2), 201–213, 1984.

Wilson, R. J. S., Anchukaitis, K., Briffa, K., Büntgen, U., Cook, E. R., D'Arrigo, R., Davi, N., Esper, J., Frank, D., Gunnarson, B., Hegerl, G., Helama, S., Klesse, S., Krusic, P. J., Linderholm, H. W., Myglan, V., Osborn, T., Rydval, M., Schneider, L., Schurer, A., Wiles, G., Zhang, P., and Zorita, E.: Last millennium northern hemisphere summer temperatures from tree rings: Part I: The long term context, Quaternary Science Reviews, 134, 1–18, 2016.

Yang, B., Qin, C., Wang, J., He, M., Melvin, T. M., Osborn, T. J., and Briffa, K. R.: A 3500-year tree-ring record of annual precipitation on the northeastern Tibetan Plateau, Proceedings of the National Academy of Sciences, 111(8), 2903-2908, 2014.

Zhang, P., Björklund, J., and Linderholm, H. W.: The influence of elevational differences in absolute maximum density values on regional climate reconstructions, Trees, 29(4), 1259–1271, 2015.

Table 1. Summary of the tree-ring MXD data.

Sampling sites	Elev	TS	NS	MSL	AMXD	MS	AC1	M-adj (g/cm^3)
Furuberget-north	650	873–1112	3	156	0.74	0.118	0.556	0
		1189–2005	61	197	0.69	0.124	0.599	0
Furuberget-south samples from the G11 study	650	1497–2008	35	193	0.64	0.133	0.457	0
Håckervalen- south	750	783–1265	30	130	0.66	0.125	0.415	0.112
		1276–1520	5	128	0.67	0.109	0.532	0.112
Håckervalen- north	650	1778–2011	5	213	0.71	0.165	0.314	0
Lilla-Rörtjärnen*	560	952–1182	13	90	0.67	0.122	0.572	0.085
		1290–1686	5	198	0.66	0.111	0.676	0.085
		1750–1861	1	112	–	–	–	0.085
Östra Helgtjärnen*	646	929–1093	6	121	0.62	0.124	0.715	-0.079
		1119–1333	3	104	0.72	0.122	0.625	-0.079
		1446–1568	2	110	0.76	0.106	0.676	-0.079
Jens Perstjärnen*	700	1196–1382	2	153	0.62	0.133	0.753	0.058
Bodsjö (historical buildings in Jämtland, Sweden) samples from the G11 study	377	1107–1291	15	158	0.84	0.082	0.676	-0.112

Elev: sampling elevation (m a.s.l.); TS: time span (years CE); NS: number of samples; MSL: mean segment length (year); AMXD: average MXD (g/cm^3); MS: mean sensitivity; AC1: first-order autocorrelation; M-adj: the adjusted values that added to each sample of the corresponding site; * indicates data from subfossil wood collected from lakes. Some of the "mean tree ages" were less than 100 years, because the MXD measurement was only a part of a tree-ring width series which was much longer. The temporal restriction of these samples was due to some parts of the samples being too rotten for MXD to be measured. MXD data from Furuberget-north, Håckervalen-south, Håckervalen-north, Lilla-Rörtjärnen, Östra Helgtjärnen and Jens Perstjärnen was not included in G11. MXD data from the historical buildings was downloaded from the International Tree-Ring Data Bank (ITRDB), and was previously used in G11.

Table 2. The calibration and verification statistics of the warm-season temperature reconstruction.

	MXD RSFi chronology		
Calibration period	1890–1950	1951–2011	1890–2011
Correlation, R	0.82[a]	0.68[a]	0.77[a]
Explained variance, R^2	0.67	0.47	0.59
No. of observations	61	61	122
Verification period	1951–2011	1890–1950	–
Explained variance, R^2	0.47	0.67	–
RE[b]	0.56	0.72	–
CE[b]	0.45	0.66	–
Slope	–	–	0.5703
Intercept	–	–	-0.1453

[a] correlation is significant at the $p < 0.01$ level; [b] RE = reduction of error; CE = coefficient of efficiency.

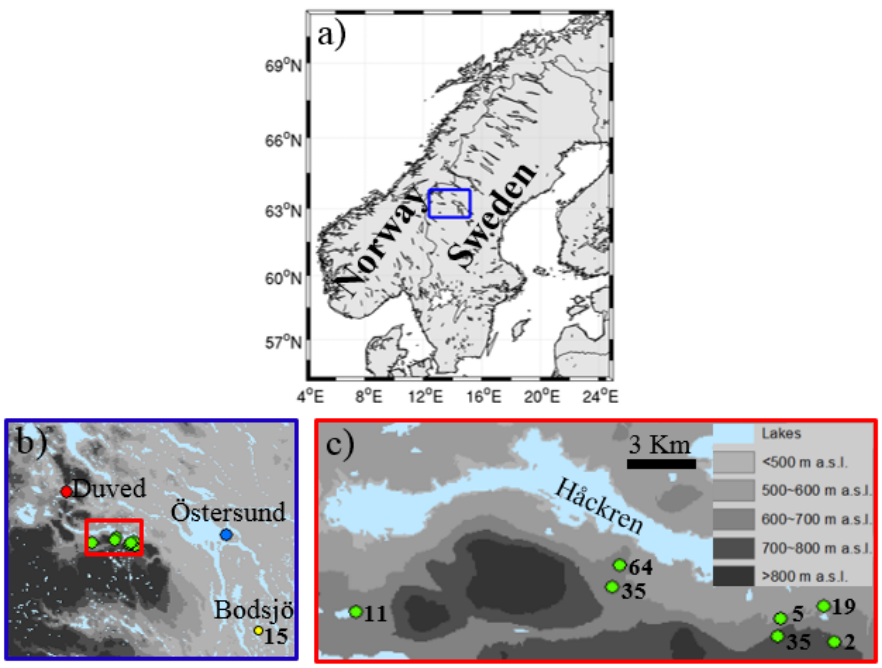

Figure 1. Map showing the locations of **(a)** the study area and **(b)** the sites of the mountain Scots pines (green dots), historical buildnings (yellow dot) samples used in this study, and the meteorological stations Duved (the red dot) and Östersund (the blue dot). **(c)** shows the topography of the mountain Scots pines. Numbers in **(b)** and **(c)** indicate the number of samples collected from each site.

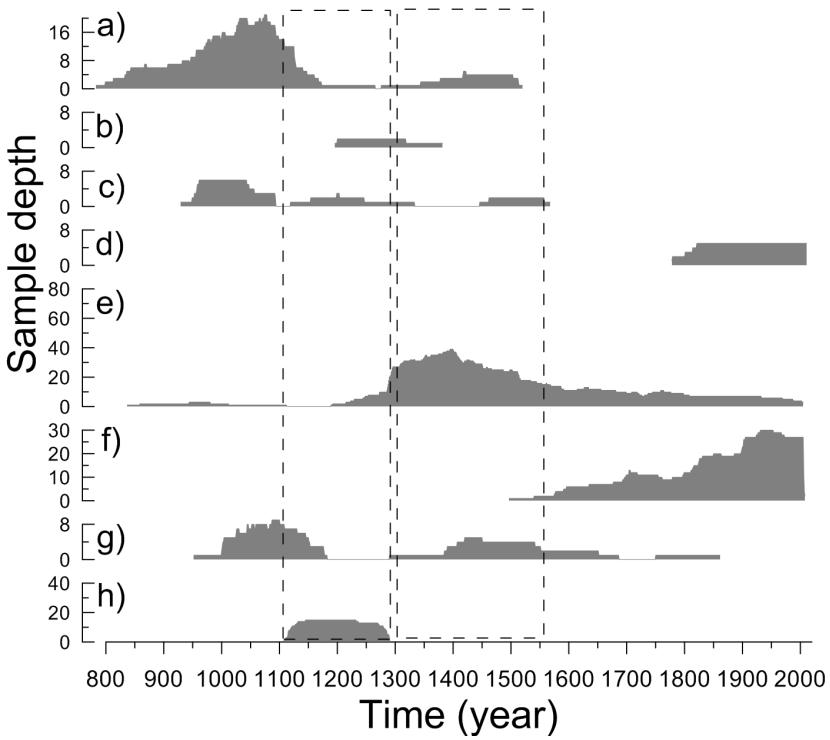

Figure 2. Sample replication through time at **(a)** Håckervalen-south, **(b)** Jens Perstjärnen, **(c)** Östra Helgtjärnen, **(d)** Håckervalen-north, **(e)** Furuberget-north, **(f)** Furuberget-south (G11), **(g)** Lilla-Rörtjärnen and **(h)** Bodsjö. The dashed lines mark the two reference periods for mean-adjustment (see main text).

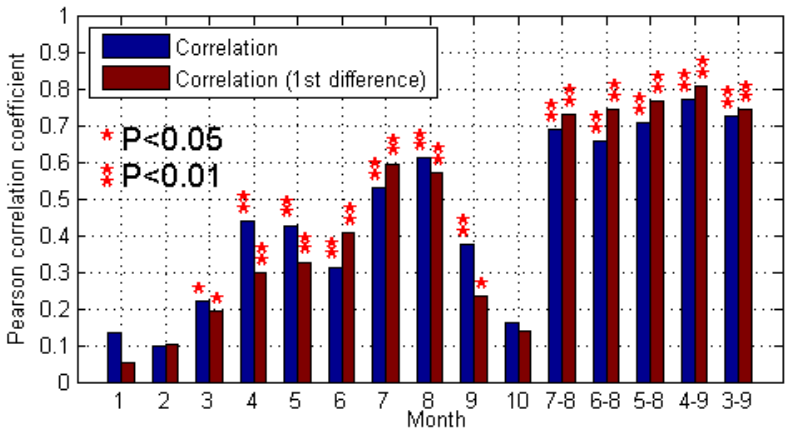

Figure 3. The correlations between the mean-adjusted MXD chronology, standardised with the RSFi method, and observed monthly mean temperatures from Duved meteorological station over the period 1890–2011. The correlations are given from January to October of the present year and July–August, June–August, May–August, April–September (warm season) and March–September means.

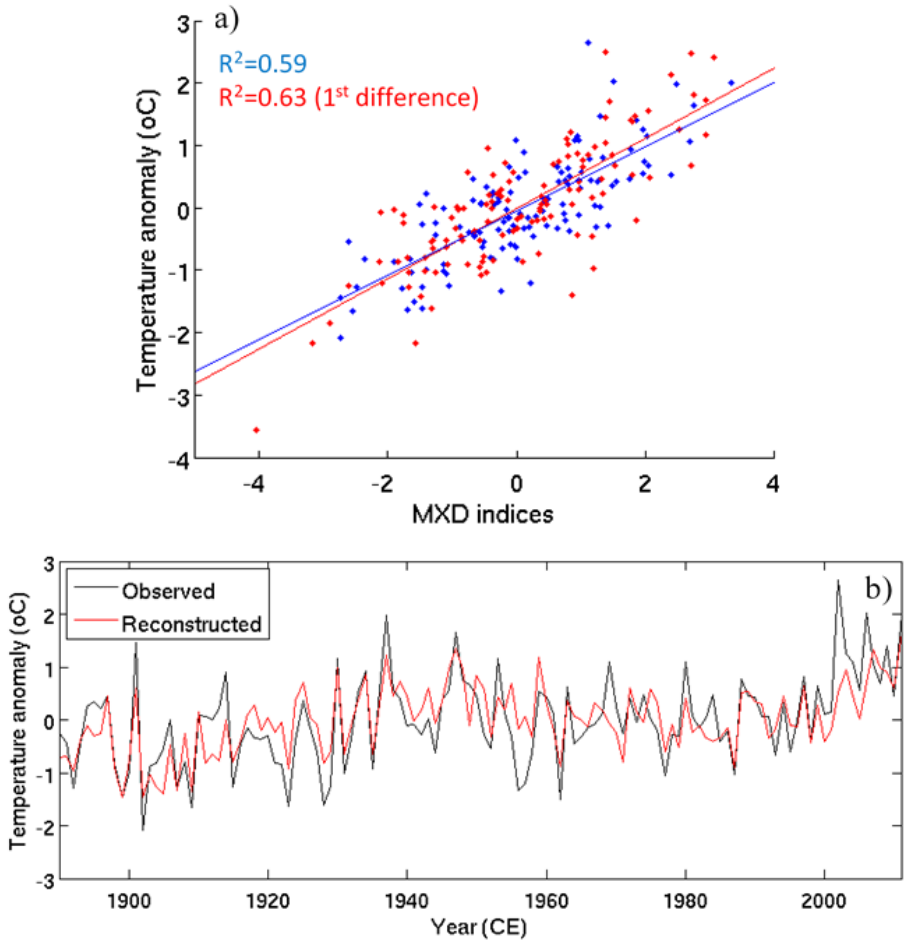

Figure 4. (a) Scatter plot of the MXD indices versus observed warm-season temperature anomalies (relative to 1961–1990 mean) from Duved (blue), and their respective 1st difference components (red), and **(b)** a comparison of reconstructed warm-season temperature (red) and observed Duved warm-season temperature (black) over the period 1890–2011.

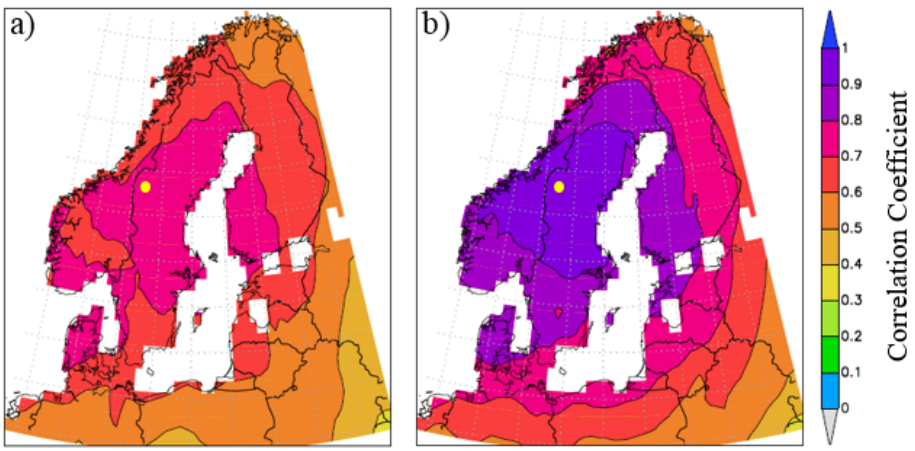

Figure 5. Field correlations between gridded warm-season temperature from the CRU TS3.23 $0.5^\circ \times 0.5^\circ$ dataset (Harris et al., 2014) during the period 1901–2011 CE and **(a)** reconstructed warm-season temperature (this study), and **(b)** observed Duved warm-season temperature. The yellow dots mark the approximate locations of the sampling sites. The field correlation maps were made using the "KNMI climate explorer" (Royal Netherlands Meteorological Institute; http://climexp.knmi.nl; van Oldenborgh et al., 2009).

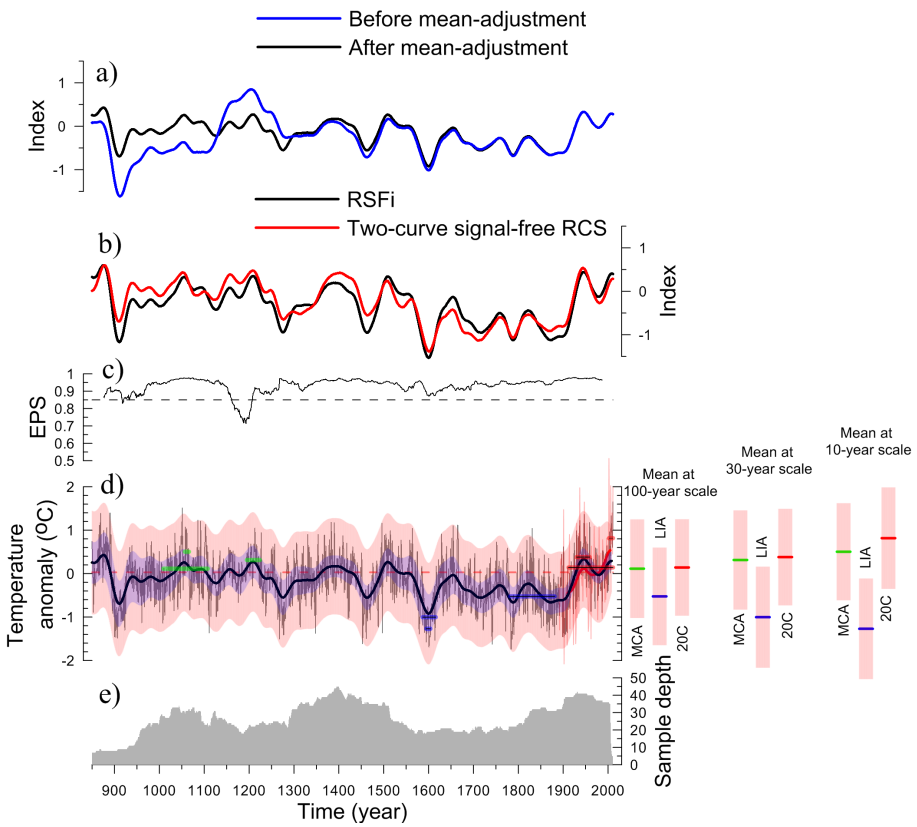

Figure 6. Characteristics of the central Scandinavian MXD chronology and the resulting warm-season temperature reconstruction: **(a)** The MXD chronologies based on samples without mean-adjustment (blue) and after mean-adjustment (black). **(b)** Comparison of the multidecadal (after 51-year Gaussian filtering) variability of the MXD chronologies standardised by the two-curve signal-free RCS standardisation method (smoothed by age-dependent spline, the red curve) and the RSFi standardisation method (fitted by age-dependent spline, the black curve). **(c)** Expressed Population Signal (EPS) through time of the chronology. The dashed line shows the 0.85 threshold. **(d)** Reconstructed annual (grey) and 51-year Gaussian filtered (bold black) warm-season temperature variability in central Scandinavia over the period 850–2011. Also indicated is the chronology uncertainty (purple shading) and the total uncertainty of the reconstruction (pink shading. This includes chronology uncertainty and reconstruction uncertainty) expressed as $+/-$ 2$\times$ the standard error. Observed warm-season temperatures are shown by the thin red (annual) and the bold red (after 51-year Gaussian filtering) curves, with the red dashed line indicating the 1961–1990 mean. The short lines to the right of panel **(d)** mark the mean temperature levels of the warmest 100, 30 and 10 years in MCA (10th-13th century (Grove and Switsur , 1994)) (green) and 20th century (red), and the coldest 100, 30 and 10 years in the LIA (14th-19th century (Grove , 2001)) (blue). The time spans are marked on the corresponding positions on the temperature curve. The coloured short lines with thin solid black line in the centre mark the time spans of the warmest and coldest 100, 30 and 10 years during the past 1200 years. **(e)** The grey shading indicates the sample depth of the MXD chronology.

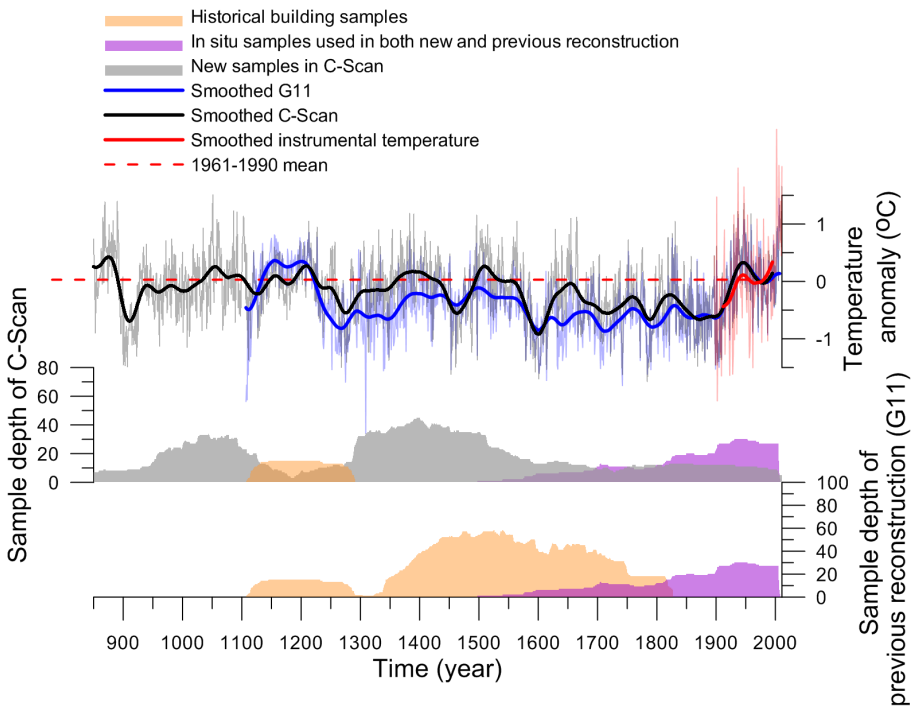

Figure 7. A comparison between C-Scan (the thin grey curve) and G11 (the thin blue curve, Gunnarson et al., 2011). Bold black and blue curves show the variability after 51-year Gaussian filtering. The sample depths of different origins used in the two reconstructions are marked by the orange, black and purple (C-Scan) and orange and purple (G11) shadings, respectively. The red curves indicate the observed year-to-year temperature variability (thin line) and its 51-year Gaussian filtered variability (thick line). The dashed red curve shows the observed 1961–1990 mean warm-season temperature.

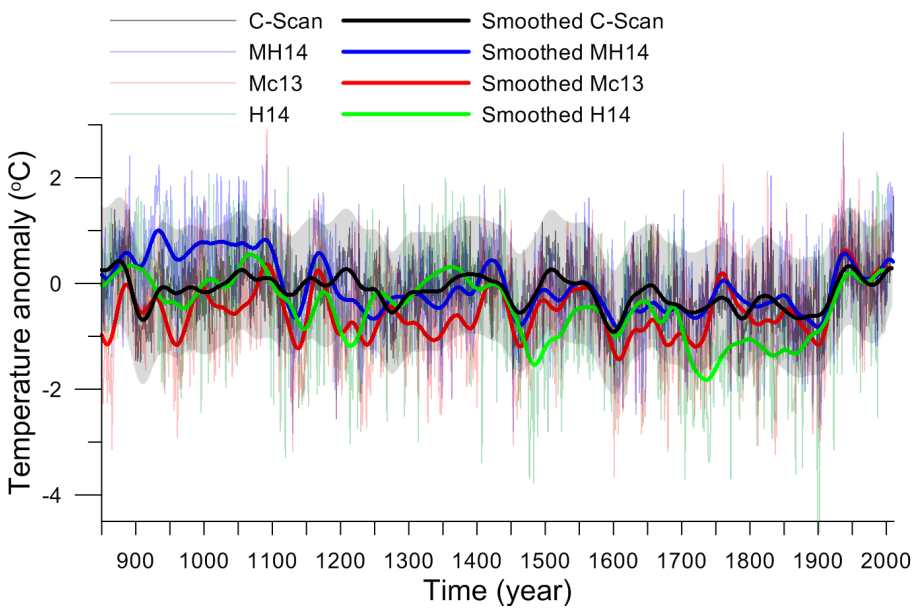

Figure 8. Comparison of temperature anomalies (from 1961–1990 period) inferred by four temperature reconstructions covering the whole last millennium: C-Scan (April–September, this study, black), MH14 (June–July, MXD, blue, Matskovsky and Helama , 2014), Mc13 (June–August, multi-proxy, red, McCarroll et al., 2013) and H14 (May–September, MXD, green, Helama et al., 2014). Bold curves show the variability after 51-year Gaussian filtering. The black shading indicates the total uncertainty of C-Scan (including chronology uncertainty and reconstruction calibration uncertainty), as expressed as $+/-$ 2$\times$ the standard error.

Appendix A

The new reconstruction, C-Scan, will be uploaded to NOAA and BALPAL, and all the data published in this study will be available for non-commercial scientific purposes.

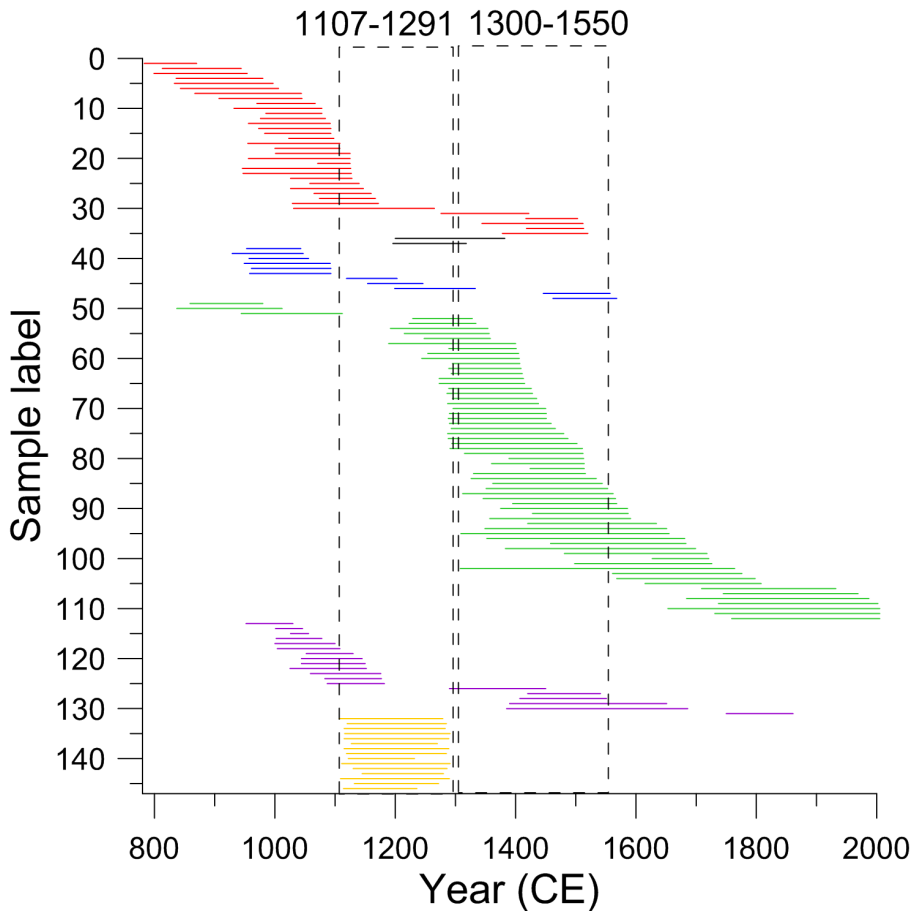

Figure A.1. The time spans of the samples from Håckervalen-south (red), Jens Perstjärnen (black), Östra Helgtjärnen (blue), Furuberget-north (green), Lilla-Rörtjärnen (purple) and Bodsjö (yellow). The samples from Furuberget-north which are fully or partly covering the period 1300–1550 are used as references for adjusting the mean values of the samples from Håckervalen-south, Jens Perstjärnen, Östra Helgtjärnen and Lilla-Rörtjärnen. The samples from Furuberget-north and the adjusted samples from Håckervalen-south, Jens Perstjärnen, Östra Helgtjärnen and Lilla-Rörtjärnen which are fully or partly covering the period 1107–1291 are used as references for adjusting the mean values of the samples from Bodsjö.

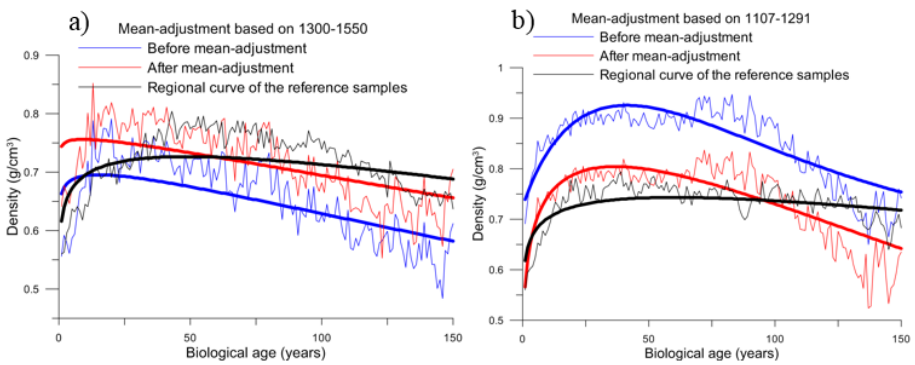

Figure A.2. (a) The smoothed (bold) and unsmoothed (thin) average growth curves of the referenced samples (from Furuberget-north, black) and the samples (from Håckervalen-south, Lilla-Rörtjärnen, Östra Helgtjärnen and Jens Perstjärnen) before (blue) and after (red) mean-adjustment in the common period (1300–1550), **(b)** the same as **(a)** but for the mean-adjustment of the historical building samples over the period 1107–1291.